Suppressed incommensurate order in swedenborgite math xmlns="http://www.w3.org/1998/Math/MathML">mrow>msub>mi>Ca/mi>mrow>mn>0.5/mn>/mrow>/msub>msub>mi mathvariant="normal">Y/mi>mrow>mn>0.5/mn>/mrow>/msub>msub>mi>BaCo/mi>mn>4/mn>/msub>msub>mi mathvariant="normal">O/mi>mn>7/mn>/msub>/mrow>/math>

Shang Gao, Vilmos Kocsis, Minoru Soda, Feng Ye, Yaohua Liu, Andrew F. May, Yasujiro Taguchi, Yoshinori Tokura, Taka-hisa Arima, Werner Schweika, Andrew D. Christianson, and Matthew B. Stone

Phys. Rev. B **104**, L140408 — Published 18 October 2021
DOI: 10.1103/PhysRevB.104.L140408

Suppressed incommensurate order in the Swedenborgite $Ca_{0.5}Y_{0.5}BaCo_4O_7$[*]

Shang Gao,[1, 2, 3, †] Vilmos Kocsis,[3, ‡] Minoru Soda,[3, 4] Feng Ye,[1] Yaohua Liu,[1] Andrew F. May,[2] Yasujiro Taguchi,[3] Yoshinori Tokura,[3, 5] Taka-hisa Arima,[3, 6] Werner Schweika,[7, 8] Andrew D. Christianson,[2] and Matthew B. Stone[1]

[1]*Neutron Scattering Division, Oak Ridge National Laboratory, Oak Ridge, TN 37831, USA*
[2]*Materials Science & Technology Division, Oak Ridge National Laboratory, Oak Ridge, TN 37831, USA*
[3]*RIKEN Center for Emergent Matter Science (CEMS), Wako 351-0198, Japan*
[4]*Department of Physics, Advanced Sciences, G.S.H.S. Ochanomizu University, Tokyo 112-8610, Japan*
[5]*Department of Applied Physics and Tokyo College, University of Tokyo, Tokyo 113-8656, Japan*
[6]*Department of Advanced Materials Science, University of Tokyo, Kashiwa 277-8561, Japan*
[7]*Jülich Center for Neutron Science JCNS and Peter Grünberg Institute PGI,*
JARA-FIT, Forschungszentrum Jülich, Jülich 52425, Germany
[8]*European Spallation Source ESS ERIC, Lund 22100, Sweden*

(Dated: October 1, 2021)

The Swedenborgite $Ca_{0.5}Y_{0.5}BaCo_4O_7$ (CYBCO) with geometrically frustrated kagomé and triangular lattices exhibits a disordered ground state in spite of strong antiferromagnetic couplings between the Co spins. The character of the disordered state has been debated due to ambiguous Co states in the triangular layers. Here we perform single-crystal diffuse neutron scattering experiments to fully characterize the short-range spin correlations in CYBCO. Through reverse Monte Carlo and self-consistent Gaussian approximation analyses, we confirm that the Co ions in both the kagomé and triangular layers are magnetic, and the interlayer couplings, together with the lattice distortion, promote an incommensurate magnetic order that is suppressed possibly by exchange disorder. Our work clarifies the short-range spin correlations in CYBCO and establishes a general correspondence between unequal interactions and incommensurate spin correlations on the Swedenborgite lattice.

In geometrically frustrated magnets, the ground state configurations exhibit an enormous degeneracy due to competing interactions, which may lead to exotic correlated states without magnetic long-range order (LRO) [1]. A prototype example is the two-dimensional antiferromagnetic Heisenberg model on the kagomé lattice (KHAFM) [2]. In the classical limit, the ground state of the KHAFM is only weakly constrained by a local zero-moment rule, leading to a classical spin-liquid state with power-law correlations [3, 4]. In real materials, however, perturbations from magnetostriction or further-neighbor interactions often relieve the degeneracy and induce magnetic LRO, making it challenging to realize a classical spin-liquid state as theoretically predicted.

The discovery of a disordered ground state in the Swedenborgite $Ca_{0.5}Y_{0.5}BaCo_4O_7$ (CYBCO) has drawn great attention [5–11]. As shown in Fig. 1(a), the Co ions in CYBCO form alternating triangular (Co1) and kagomé (Co2) layers in the *ab* plane. Although magnetization measurements reveal a Curie-Weiss temperature of −2200 K suggesting strong antiferromagnetic (AF) couplings between the Co spins, LRO has not been detected by neutron diffraction down to 1.2 K [5, 6]. As the powder-averaged magnetic diffuse scattering closely resembles the KHAFM spin-liquid state [12], it is proposed that the Co1 ions in the triangular layers may be

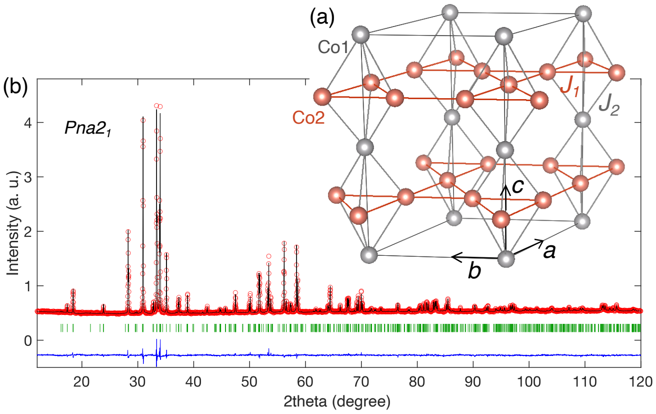

FIG. 1. (a) The Co ions in CYBCO form a lattice of alternating triangular (Co1) and kagomé (Co2) layers in the *ab* plane. The crystal structure is shown in the hexagonal unit cell. J_1 (J_2) denotes the couplings within the kagomé layers (between the kagomé and triangular layers). (b) Refinement results of the XRD data measured at room temperature for pulverized CYBCO crystals. Data points are shown as red circles. The calculated pattern is shown as the black solid line. The vertical bars show the positions of the Bragg peaks for CYBCO with space group $Pna2_1$. The blue line at the bottom shows the difference of measured and calculated intensities.

---

[*] This manuscript has been authored by UT-Battelle, LLC under Contract No. DE-AC05-00OR22725 with the U.S. Department of Energy. The United States Government retains and the publisher, by accepting the article for publication, acknowledges that the United States Government retains a non-exclusive, paid-up, irrevocable, world-wide license to publish or reproduce the published form of this manuscript, or allow others to do so, for United States Government purposes. The Department of Energy will provide public access to these results of federally sponsored research in accordance with the DOE Public Access Plan (http://energy.gov/downloads/doe-public-access-plan).

[†] gaos2@ornl.gov

[‡] Current address: Institut für Festkörperforschung, Leibniz IFW Dresden, 01069 Dresden, Germany

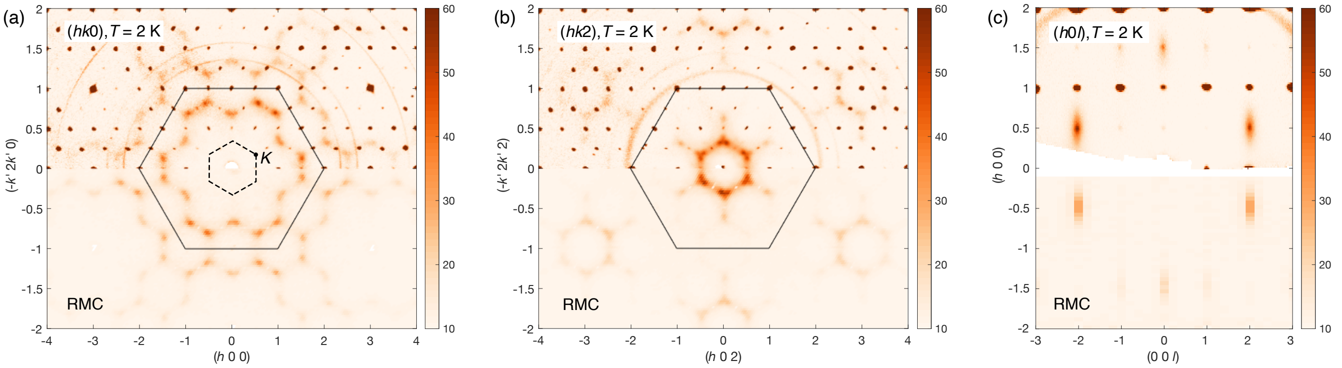

FIG. 2. Short-range spin correlations in CYBCO in the (a) ($hk0$), (b) ($hk2$), and (c) ($h0l$) planes. In each panel, the upper half is the experimental data collected on CORELLI at 2 K, and the lower half is the calculated spin correlations from the RMC simulations. In panels (a) and (b), the solid line indicates the periodicity of the diffuse scattering pattern in the ($hk0$) and ($hk2$) planes. In panel (a), the dashed line outlines the first Brillouin zone boundary with the $K(\frac{1}{3}\frac{1}{3}0)$ point indicated. The additional ring-like scattering in the experimental data arises from the sample environment.

of the nonmagnetic $S = 0$ Co^{3+} configuration so that the Co2 spins realize a KHAFM [6]. However, more recent reverse Monte Carlo (RMC) analysis of the powder neutron scattering data suggests an extrinsic scenario where both the Co1 and Co2 ions are magnetic and the LRO is mainly suppressed by the exchange disorder between the Co spins in the presence of randomly distributed Ca and Y ions [13, 14]. A single crystal study is needed to directly resolve the spin correlations in reciprocal space and unambiguously determine the origin of the disordered state in CYBCO.

Here we report our diffuse neutron scattering study of a CYBCO crystal. Strong modulation of the spin correlations along the c axis is observed, which indicates a nonzero interlayer coupling that is confirmed in our RMC and self-consistent Gaussian approximation (SCGA) analyses. In the ab plane, incommensurate spin correlations are observed. By comparing the spin correlations under different perturbations, we are able to ascribe the incommensurability to unequal exchange interactions that can be induced by lattice distortions. Our work clarifies the ground state of CYBCO as an incipient incommensurate magnetic order that is suppressed by exchange disorder, and establishes a general correspondence between unequal interactions and incommensurate spin correlations on the Swedenborgite lattice.

Single crystals of CYBCO were grown by the floating zone method [5, 15]. Details for the sample preparation and basic characterizations can be found in the Supplementary Materials [16] (see, also, references [17–25] therein). Figure 1(b) summarizes the refinement results of the X-ray diffraction (XRD) data collected at room temperature on pulverized CYBCO crystals. Our diffraction data reveal the space group to be orthorhombic $Pna2_1$, which is the same as that of the parent compounds $\mathrm{CaBaCo_4O_7}$ [26–28] and $\mathrm{YBaCo_4O_7}$ [29] at room temperature, but different from the hexagonal $P6_3mc$ [5, 6] or trigonal $P31c$ [13] space group reported previously. Such a difference may arise from the variance in the oxygen content [30], which is determined to be $\mathrm{O}_{7.14(6)}$ in our annealed crystals through thermalgravimetric analysis (TGA). The weak orthorhombic distortion causes a $\sim$ 0.4% shrinkage along the a axis from the hexagonal symmetry [31]. The Ca and Y ions are randomly distributed over the same site with a fractional weight of 0.52(1) and 0.48(1), respectively. The complete refined structural parameters are summarized in the Supplementary Materials [16].

To characterize the short-range spin correlations in CYBCO, we perform single-crystal diffuse neutron scattering experiments on the CORELLI elastic diffuse scattering spectrometer at the Spallation Neutron Source (SNS), Oak Ridge National Laboratory [16, 32]. The top half of Fig. 2 presents the representative scattering patterns in the ($hk0$), ($hk2$), and ($h0l$) planes measured at $T = 2$ K, well below the successive spin freezing transition temperatures of $\sim$ 15, 50, and 250 K observed in magnetic susceptibility [5, 16]. Indices in the diffuse patterns are denoted in the hexagonal system for convenience. The nuclear Bragg peaks with half integer indices are consistent with the orthorhombic distortion, while the broad diffuse signal is in agreement with the absence of magnetic LRO as previously reported [6, 13]. However, the diffuse scattering intensities are strongly modulated along the c axis: intensities are concentrated in the planes with integer l as revealed in Fig. 2(c); and the scattering patterns in ($hk0$) and ($hk2$) are very different. These observations are not consistent with defining CYBCO as a KHAFM system because the spin correlations in a KHAFM exhibit no modulation out of the kagomé plane. Instead, the observed diffuse patterns, especially the relatively narrow peak width along ($0\ 0\ l$), are more similar to the quasi-one-dimensional order observed in $\mathrm{YBaCo_4O_7}$ that arises from the relatively strong interlayer couplings [33].

RMC analysis was performed to fit the diffuse signal over volumes in reciprocal space [16, 34, 35]. This is a model-free method that allows the spin-spin correla-

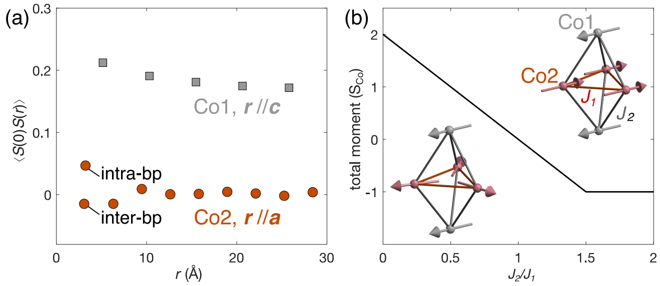

FIG. 3. (a) Spin correlations $\langle \boldsymbol{S}(0)\boldsymbol{S}(\boldsymbol{r})\rangle$ as a function of distance r calculated through RMC. Gray squares (red circles) are the correlations for the Co1 (Co2) spins along the c (a) axis. For the first-neighbor Co2 spins at $r \sim 3.2$ Å, correlations within the bipyramids (intra-bp) and out of the bipyramids (inter-bp) are calculated separately. Error bars representing the standard deviations are smaller than the size of the symbol. (b) Total moment of the spin bipyramid as a function of J_2/J_1. Insets are representative ground states for infinitely small J_2/J_1 (left) and $J_2/J_1 \geq 1.5$ (right).

tions to be extracted and subsequently used as a starting point to construct an effective spin Hamiltonian. Considering the strong modulation of the diffuse scattering intensity along the c axis, both the Co1 and Co2 ions are assumed to be magnetic with an equal moment size of $S = 3/2$ [13, 14]. As shown in Fig. 2, our RMC simulations reproduce the intensity distributions in reciprocal space, including the disparate patterns in the ($hk0$) and ($hk2$) planes together with the quasi-one-dimensional order along the c axis. The representatives of the extracted spin-spin correlations $\langle \boldsymbol{S}_i \cdot \boldsymbol{S}_j\rangle$ in real space are summarized in Fig. 3(a). The interlayer correlations between the Co1 spins are higher than ~ 0.17 even at a large separation of 5 layers (~ 26 Å) and are thus of a FM character. In contrast, the in-plane correlations of the Co2 spins along the a axis decay rapidly to zero at increasing distances. Interestingly, the Co2 spins in the bipyramid units (intra-bp) exhibit FM correlations, which appears to be contradictory with the AF couplings in the kagomé layers.

The bipyramid unit of the Swedenborgite lattice with antiferromagnetically coupled spins provides a qualitative explanation for the observed correlations [8, 10, 33]. Assuming the in-plane and out-of-plane couplings to be J_1 and J_2, respectively, Fig. 3(b) shows the total moment of the bipyramid unit in the ground state as a function of J_2/J_1. Even at infinitesimal J_2, the total moment is close to $2S_{\mathrm{Co}}$, meaning the two apical Co1 spins tend to be parallel, which explains the FM correlations among the Co1 spins along the c axis. For increasing J_2/J_1, the Co1 spins stay parallel, while the three Co2 spins in the basal plane gradually change from an AF 120° configuration at $J_2 = 0$ to a parallel configuration at $J_2 \geq 1.5J_1$. Thus our observed FM correlations for the Co2 spins within the bipyramid units is consistent the AF J_1 couplings in the kagomé layers if relatively strong AF interlayer couplings J_2 are considered.

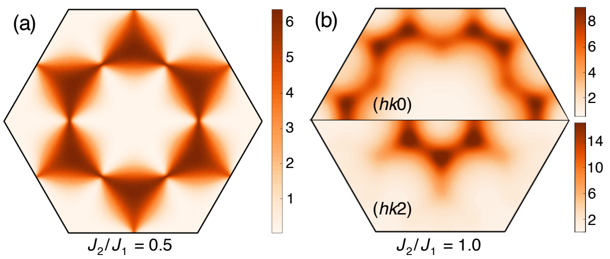

FIG. 4. The diffuse neutron scattering pattern in the ($hk0$) plane calculated through the SCGA method for $J_2/J_1 = 0.5$ at reversed temperature $\beta = 100$ (a) and in ($hk0$) and ($hk2$) planes calculated for $J_2/J_1 = 1.0$ at $\beta = 4.5$ (b). The hexagon outlines the same region as the solid hexagon in Fig. 2. Pinch-points arising from the flat eigenbands disappear at $J_2/J_1 > \sqrt{2}/2$, giving rise to a pattern that is similar to the experimental results.

Similar conclusions can also be drawn with a lattice model that incorporates the J_1 and J_2 couplings. Starting from the Hamiltonian $\mathcal{H} = J_1 \sum_{ij\in 1} \boldsymbol{S}_i\boldsymbol{S}_j + J_2 \sum_{ij\in 2} \boldsymbol{S}_i\boldsymbol{S}_j$, we explore the short-range spin correlations using the SCGA method [16, 36–41]. At $J_2 = 0$, the J_1-J_2 model is equivalent to the KHAFM, where the spin correlations are well understood in the classical regime [3, 4]. The interaction matrix of the KHAFM has a flat eigenband at the bottom [16], indicating the absence of magnetic order at mean-field level. When spin fluctuations are considered, a correlated paramagnetic phase with dipolar-like spin correlations will emerge, which is signified by pinch points in the diffuse scattering pattern [3, 42]. As presented in Fig. 4(a), a similar correlated paramagnetic phase is realized on the Swedenborgite lattice for $J_2/J_1 < \sqrt{2}/2$ [8]. Above this threshold, the eigenband at the bottom becomes dispersive [8, 16], indicating the existence of a magnetic order at mean-field level. Figure 4(b) presents the diffuse scattering patterns calculated by the SCGA method at $J_2/J_1 = 1$ that is representative for the $J_2/J_1 \geq \sqrt{2}/2$ regime [8]. The intensity distribution is very different from that of the KHAFM in Fig. 4(a), but reproduces the main features observed in CYBCO as shown in Fig. 2. Thus, via both the RMC and the SCGA calculations, the existence of the interlayer couplings J_2 in CYBCO is unambiguously established.

For the J_1-J_2 Heisenberg model on the Swedenborgite lattice, the magnetic LRO predicted in the mean-field theory can be removed by spin fluctuations, which increases the ordering threshold to $J_2/J_1 = 3/2$ according to classical Monte Carlo simulations [8, 10]. As the diffuse scattering patterns at elevated temperatures are similar on both sides of the threshold, the J_1-J_2 model cannot distinguish whether the disordered ground state in CYBCO is intrinsic due to spin fluctuations or extrinsic due to exchange disorder.

A closer look at the experimental and calculated patterns allows us to differentiate the intrinsic and extrin-

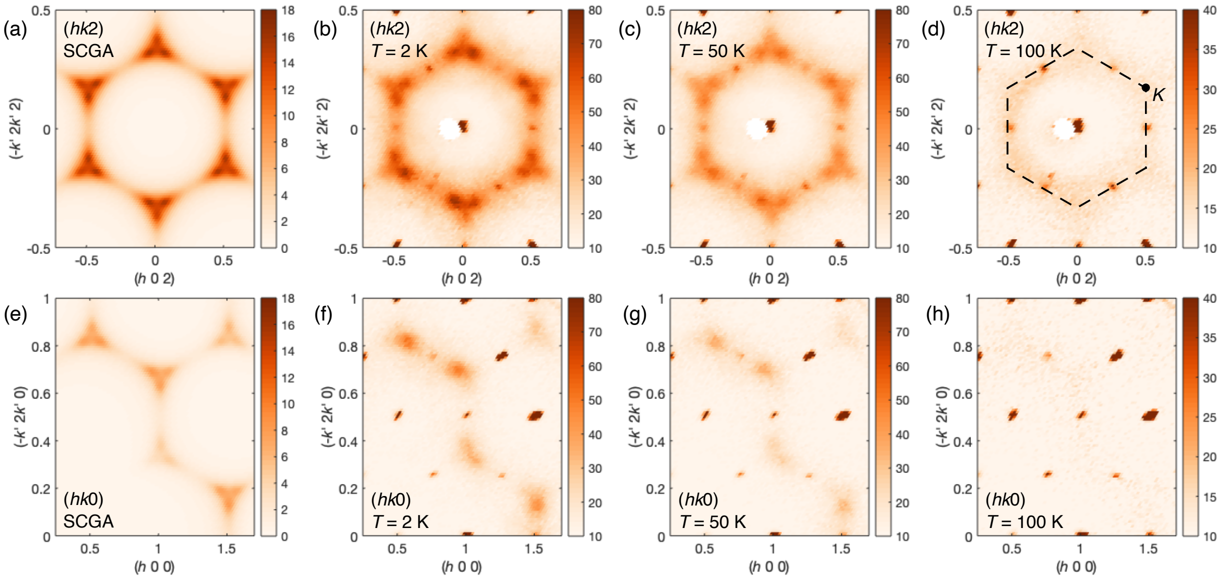

FIG. 5. Diffuse neutron scattering pattern in the $(hk2)$ plane (a) and $(hk0)$ plane (e) calculated by the SCGA method using a J_{1a}-J_{1b}-J_{1c}-J_2 model at $\beta = 3.2$, where $J_{1a} = 0.9$, $J_{1b} = 1.0$, and $J_{1c} = 1.1$ are the distinctive first-neighbor couplings in the kagomé layer due to lattice distortion. The calculated intensities are averaged over equally populated domains. Zoomed-in plot for the experimental diffuse scattering patterns in the $(hk2)$ plane (b-d) and $(hk0)$ plane (f-h). Data were collected at 2 K (b, f), 50 K (c, g), and 100 K (d, h). Dashed line in panel (d) outlines the first Brillouin zone boundary.

sic scenarios. Although the J_1-J_2 model reproduces the main features of the diffuse scattering pattern, it fails to capture the details around K, $(\frac{1}{3}\frac{1}{3}0)$, and its equivalent points. As shown in Fig. 2 (also see Fig. 5 for greater detail), the maxima of the diffuse scattering intensities are slightly shifted from the K points along the Brillouin zone boundary, revealing incommensurate spin correlations that are not predicted by the J_1-J_2 model. Although similar incommensurate correlations have been observed in the Swedenborgites, e.g. $\mathrm{LuBaCo_4O_7}$ [43, 44] and $\mathrm{CaBaCo_2Fe_2O_7}$ [45], their microscopic origins are unclear and the perturbation terms to the J_1-J_2 Hamiltonian still remain to be determined. If the perturbation terms further relieve the ground state degeneracy, the disordered ground state in CYBCO is more likely extrinsic due to exchange disorder as proposed in Ref. [13].

To understand the origin of incommensurate spin correlations in CYBCO and the related compounds, we first explore the perturbations from Dzyaloshinskii-Moriya interactions (DMI) and further-neighbor exchange interactions. As discussed in the Supplementary Materials [16], a variety of diffuse patterns are observed under perturbations, although none of them exhibits incommensurate correlations as observed in our experiment. This suggests the necessity of perturbations other than DMI or further-neighbor couplings.

Since the orthorhombic lattice distortion breaks the three-fold rotation symmetry along the c axis, we next consider a minimal J_{1a}-J_{1b}-J_{1c}-J_2 model with unequal J_1 coupling strengths in the kagomé layers. It is noteworthy that unequal interactions may also arise from local distortions due to chemical disorder even in the absence of a uniform lattice distortion. The diffuse patterns calculated by the SCGA method with $J_{1a} = 0.9$, $J_{1b} = 1.0$, $J_{1c} = 1.1$, and $J_2 = 1.0$ are shown in Fig. 5 together with the temperature evolution of the experimental data. After averaging over the orthorhombic domains, our minimal model successfully reproduces the incommensurate correlations. The slight mismatch around the K points in the $(hk0)$ plane may arise from unequal domain populations or further perturbations that are not considered in our minimal model. Similar incommensurate correlations are obtained by introducing unequal J_2 couplings. Our calculations thus reveal the importance of unequal couplings in stabilizing incommensurate spin correlations in CYBCO and the related compounds. Furthermore, as unequal interactions relieve the ground state degeneracy and result in a magnetic LRO transition at $T_N \sim 0.3J_1$ in our minimal model, we are able to conclude that the disordered ground state in CYBCO is more likely extrinsic due to exchange disorder.

The temperature dependence of the diffuse pattern also supports the extrinsic origin of the suppressed order in CYBCO. As shown in Fig. 5, the intensity distribution, including the relative strengths of the incommensurate satellites, stays almost constant below $\sim$ 50 K. Such a weak temperature dependence contradicts the intrinsic spin-liquid state predicted for $J_2/J_1 < 1.5$ [8, 10]. Instead, it implies a spin freezing scenario where the short-range spin correlations are prevented from developing into a LRO due to exchange disorder [13]. The extrinsic scenario is further corroborated by comparing the spin correlations in the related Swedenborgites, as an AF LRO has been observed in both the parent compounds

$YBaCo_4O_7$ [15, 29, 44, 46–48] and $CaBaCo_4O_7$ [26–28, 31, 49].

Although the discovery of the magnetoelectric effect in $CaBaCo_4O_7$ has drawn great attention to this family of compounds [27, 50–54], the effect of local or lattice distortion on the spin correlations has remained barely explored. Therefore, the correspondence between unequal interactions and incommensurate spin correlations established in our work should have broad impacts on understanding the magnetic and magneto-electric properties of the Swedenborgites. Especially, for the doped Swedenborgites, similar incommensurate spin correlations may emerge due to local distortions induced by chemical disorder even without a uniform lattice distortion [55–57].

We have shown that the previously proposed intrinsic scenario of uncoupled kagomé layers in the swedenborgites is not consistent with our single-crystal diffuse neutron scattering experiments. Rather we determine the disordered ground state in CYBCO to be an incipient incommensurate magnetic order that is suppressed by exchange disorder. By comparing the spin correlations on the Swedenborgite lattice under different perturbations, we are able to explain the incommensurate spin correlations in CYBCO by unequal interactions that are induced by lattice distortion. This correspondence between unequal interactions and incommensurate spin correlations can be applied to other Swedenborgite family of compounds.

ACKNOWLEDGMENTS

We acknowledge discussions with Raphaël Hermann, Joseph Paddison, and assistance from Jie Xing and Jia-Qiang Yan. This work was supported by the U.S. Department of Energy, Office of Science, Basic Energy Sciences, Materials Sciences and Engineering Division. This research used resources at the Spallation Neutron Source (SNS), a DOE Office of Science User Facilities operated by the Oak Ridge National Laboratory (ORNL).

[1] L. Balents, Spin liquids in frustrated magnets, Nature **464**, 199 (2010).
[2] J. T. Chalker, P. C. W. Holdsworth, and E. F. Shender, Hidden order in a frustrated system: Properties of the Heisenberg kagom antiferromagnet, Phys. Rev. Lett. **68**, 855 (1992).
[3] D. A. Garanin and B. Canals, Classical spin liquid: Exact solution for the infinite-component antiferromagnetic model on the kagomé lattice, Phys. Rev. B **59**, 443 (1999).
[4] M. Taillefumier, J. Robert, C. L. Henley, R. Moessner, and B. Canals, Semiclassical spin dynamics of the antiferromagnetic Heisenberg model on the kagome lattice, Phys. Rev. B **90**, 064419 (2014).
[5] M. Valldor, Remnant magnetization above room temperature in the semiconductor $Y_{0.5}Ca_{0.5}BaCo_4O_7$, Solid State Sci. **8**, 1272 (2006).
[6] W. Schweika, M. Valldor, and P. Lemmens, Approaching the ground state of the kagomé antiferromagnet, Phys. Rev. Lett. **98**, 067201 (2007).
[7] M. E. Zhitomirsky, Octupolar ordering of classical kagome antiferromagnets in two and three dimensions, Phys. Rev. B **78**, 094423 (2008).
[8] D. D. Khalyavin, P. Manuel, J. F. Mitchell, and L. C. Chapon, Spin correlations in the geometrically frustrated $RBaCo_4O_7$ antiferromagnets: Mean-field approach and Monte Carlo simulations, Phys. Rev. B **82**, 094401 (2010).
[9] S. Buhrandt and L. Fritz, Antiferromagnetic Ising model on the swedenborgite lattice, Phys. Rev. B **90**, 094415 (2014).
[10] S. Buhrandt and L. Fritz, Spin-liquid phase and order by disorder of classical Heisenberg spins on the swedenborgite lattice, Phys. Rev. B **90**, 020403(R) (2014).
[11] T. S. Sikkenk, K. Coester, S. Buhrandt, L. Fritz, and K. P. Schmidt, Emergence of a two-dimensional macrospin liquid in a highly frustrated three-dimensional quantum magnet, Phys. Rev. B **95**, 060401(R) (2017).
[12] J. N. Reimers and A. J. Berlinsky, Order by disorder in the classical heisenberg kagomé antiferromagnet, Phys. Rev. B **48**, 9539 (1993).
[13] J. R. Stewart, G. Ehlers, H. Mutka, P. Fouquet, C. Payen, and R. Lortz, Spin dynamics, short-range order, and spin freezing in $Y_{0.5}Ca_{0.5}BaCo_4O_7$, Phys. Rev. B **83**, 024405 (2011).
[14] J. A. M. Paddison, J. R. Stewart, and A. L. Goodwin, Spinvert: a program for refinement of paramagnetic diffuse scattering data, J. Phys.: Condensed Matt. **25**, 454220 (2013).
[15] M. Soda, Y. Yasui, T. Moyoshi, M. Sato, N. Igawa, and K. Kakurai, Magnetic structure of $YBaCo_4O_7$ with kagome and triangular lattices, J. Phys. Society Jpn. **75**, 054707 (2006).
[16] See Supplemental Materials for experimental and theoretical methods, basic characterizations of the sample, and spin correlations perturbed by DMI and further-neighbor couplings.
[17] S. Toth and B. Lake, Linear spin wave theory for single-Q incommensurate magnetic structures, J. Phys.: Condensed Matt. **27**, 166002 (2015).
[18] A. Huq, J. Mitchell, H. Zheng, L. Chapon, P. Radaelli, K. Knight, and P. Stephens, Structural and magnetic properties of the Kagomé antiferromagnet $YbBaCo_4O_7$, J. Solid State Chem. **179**, 1136 (2006).
[19] D. Bergman, J. Alicea, E. Gull, S. Trebst, and L. Balents, Order-by-disorder and spiral spin-liquid in frustrated diamond-lattice antiferromagnets, Nat. Phys. **3**, 487 (2007).
[20] S. Gao, O. Zaharko, V. Tsurkan, Y. Su, J. S. White, G. S. Tucker, B. Roessli, F. Bourdarot, R. Sibille, D. Chernyshov, T. Fennell, A. Loidl, and C. Rüegg, Spiral spin-liquid and the emergence of a vortex-like state in $MnSc_2S_4$, Nat. Phys. **13**, 157 (2017).
[21] O. Arnold, J. Bilheux, J. Borreguero, A. Buts, S. Campbell, L. Chapon, M. Doucet, N. Draper, R. Ferraz Leal, M. Gigg, V. Lynch, A. Markvardsen, D. Mikkel-

son, R. Mikkelson, R. Miller, K. Palmen, P. Parker, G. Passos, T. Perring, P. Peterson, S. Ren, M. Reuter, A. Savici, J. Taylor, R. Taylor, R. Tolchenov, W. Zhou, and J. Zikovsky, MantidData analysis and visualization package for neutron scattering and μSR experiments, Nucl. Instr. Methods Phys. Res. Sec. A **764**, 156 (2014).

[22] J. Rodriguez-Carvajal, Recent advances in magnetic structure determination by neutron powder diffraction, Physica B: Conden. Matter **192**, 55 (1993).

[23] M. Enjalran and M. J. P. Gingras, Theory of paramagnetic scattering in highly frustrated magnets with long-range dipole-dipole interactions: The case of the $Tb_2Ti_2O_7$ pyrochlore antiferromagnet, Phys. Rev. B **70**, 174426 (2004).

[24] A. Mulder, R. Ganesh, L. Capriotti, and A. Paramekanti, Spiral order by disorder and lattice nematic order in a frustrated Heisenberg antiferromagnet on the honeycomb lattice, Phys. Rev. B **81**, 214419 (2010).

[25] T. Sarkar, V. Pralong, and B. Raveau, Formation of magnetic glass in calcium-doped $YBaCo_2O_{5.5}$ cobaltites, Phys. Rev. B **83**, 214428 (2011).

[26] V. Caignaert, V. Pralong, A. Maignan, and B. Raveau, Orthorhombic kagome cobaltite $CaBaCo_4O_7$: A new ferrimagnet with a T_C of 70 K, Solid State Commun. **149**, 453 (2009).

[27] V. Caignaert, A. Maignan, K. Singh, C. Simon, V. Pralong, B. Raveau, J. F. Mitchell, H. Zheng, A. Huq, and L. C. Chapon, Gigantic magnetic-field-induced polarization and magnetoelectric coupling in a ferrimagnetic oxide $CaBaCo_4O_7$, Phys. Rev. B **88**, 174403 (2013).

[28] J. Lohr, A. L. Larralde, J. Curiale, R. Sánchez, J. Campo, G. J. Cuello, D. Sheptyakov, L. Keller, M. Kenzelmann, and G. Aurelio, Intermediate magnetic phase of the magnetoelectric compound (Ca,Sr)$BaCo_4O_7$ described with the superspace formalism, Phys. Rev. B **102**, 134406 (2020).

[29] D. D. Khalyavin, P. Manuel, B. Ouladdiaf, A. Huq, P. W. Stephens, H. Zheng, J. F. Mitchell, and L. C. Chapon, Spin-ordering and magnetoelastic coupling in the extended kagome system $YBaCo_4O_7$, Phys. Rev. B **83**, 094412 (2011).

[30] Z. A. Kazei, V. V. Snegirev, L. P. Kozeeva, M. Y. Kameneva, and A. N. Lavrov, Effect of oxygen nonstoichiometry on the magnetic phase transitions in frustrated $YBaCo_4O_{7+x}$ (x = 0, 0.1, 0.2) cobaltites, J. Exp. Theor. Phys. **126**, 650 (2018).

[31] T. Omi, Y. Watanabe, N. Abe, H. Sagayama, A. Nakao, K. Munakata, Y. Tokunaga, and T.-h. Arima, Antiferromagnetic-to-ferrimagnetic phase transition with large electric-polarization change in a frustrated polar magnet $CaBaCo_4O_7$, Phys. Rev. B **103**, 184412 (2021).

[32] F. Ye, Y. Liu, R. Whitfield, R. Osborn, and S. Rosenkranz, Implementation of cross correlation for energy discrimination on the time-of-flight spectrometer CORELLI, J. Appl. Cryst. **51**, 315 (2018).

[33] P. Manuel, L. C. Chapon, P. G. Radaelli, H. Zheng, and J. F. Mitchell, Magnetic correlations in the extended kagome $YBaCo_4O_7$ probed by single-crystal neutron scattering, Phys. Rev. Lett. **103**, 037202 (2009).

[34] D. A. Keen and R. L. McGreevy, Determination of disordered magnetic structures by RMC modelling of neutron diffraction data, J. Phys.: Condensed Matt. **3**, 7383 (1991).

[35] J. A. M. Paddison, M. J. Gutmann, J. R. Stewart, M. G. Tucker, M. T. Dove, D. A. Keen, and A. L. Goodwin, Magnetic structure of paramagnetic MnO, Phys. Rev. B **97**, 014429 (2018).

[36] P. H. Conlon and J. T. Chalker, Absent pinch points and emergent clusters: Further neighbor interactions in the pyrochlore Heisenberg antiferromagnet, Phys. Rev. B **81**, 224413 (2010).

[37] P. H. Conlon, *Aspects of frustrated magnetism*, Ph.D. thesis, University of Oxford (2010).

[38] S. Tóth, K. Rolfs, A. R. Wildes, and C. Rüegg, Strong exchange anisotropy in $YbMgGaO_4$ from polarized neutron diffraction (2017), arXiv:1705.05699 [cond-mat.str-el].

[39] X. Bai, J. A. M. Paddison, E. Kapit, S. M. Koohpayeh, J.-J. Wen, S. E. Dutton, A. T. Savici, A. I. Kolesnikov, G. E. Granroth, C. L. Broholm, J. T. Chalker, and M. Mourigal, Magnetic excitations of the classical spin liquid $MgCr_2O_4$, Phys. Rev. Lett. **122**, 097201 (2019).

[40] J. A. M. Paddison, Scattering signatures of bond-dependent magnetic interactions, Phys. Rev. Lett. **125**, 247202 (2020).

[41] X.-P. Yao, J. Q. Liu, C.-J. Huang, X. Wang, and G. Chen, Generic spiral spin liquids, Front. Phys. **16**, 53303 (2021).

[42] T. Fennell, P. P. Deen, A. R. Wildes, K. Schmalzl, D. Prabhakaran, A. T. Boothroyd, R. J. Aldus, D. F. McMorrow, and S. T. Bramwell, Magnetic Coulomb phase in the spin ice $Ho_2Ti_2O_7$, Science **326**, 415 (2009).

[43] M. Soda, T. Moyoshi, Y. Yasui, M. Sato, and K. Kakurai, Successive phase transitions of $LuBaCo_4O_7$ with kagome and triangular lattices, J. Phys. Society Jpn. **76**, 084701 (2007).

[44] M. Soda, K. Morita, G. Ehlers, F. Ye, T. Tohyama, H. Yoshizawa, T. Masuda, and H. Kawano-Furukawa, Magnetic diffuse scattering of $YBaCo_4O_7$ and $LuBaCo_4O_7$ on kagome and triangular lattices, J. Phys. Society Jpn. **90**, 074704 (2021).

[45] J. D. Reim, E. Rosén, O. Zaharko, M. Mostovoy, J. Robert, M. Valldor, and W. Schweika, Neutron diffraction study and theoretical analysis of the antiferromagnetic order and the diffuse scattering in the layered kagome system $CaBaCo_2Fe_2O_7$, Phys. Rev. B **97**, 144402 (2018).

[46] M. Valldor and M. Andersson, The structure of the new compound $YBaCo_4O_7$ with a magnetic feature, Solid State Sci. **4**, 923 (2002).

[47] L. C. Chapon, P. G. Radaelli, H. Zheng, and J. F. Mitchell, Competing magnetic interactions in the extended kagomé system $YBaCo_4O_7$, Phys. Rev. B **74**, 172401 (2006).

[48] M. Soda, S. Itoh, T. Yokoo, G. Ehlers, H. Kawano-Furukawa, and T. Masuda, Magnetic correlations in $YBaCo_4O_7$ on kagome and triangular lattices, Phys. Rev. B **101**, 214444 (2020).

[49] V. Caignaert, V. Pralong, V. Hardy, C. Ritter, and B. Raveau, Magnetic structure of $CaBaCo_4O_7$: Lifting of geometrical frustration towards ferrimagnetism, Phys. Rev. B **81**, 094417 (2010).

[50] K. Singh, V. Caignaert, L. C. Chapon, V. Pralong, B. Raveau, and A. Maignan, Spin-assisted ferroelectricity in ferrimagnetic $CaBaCo_4O_7$, Phys. Rev. B **86**, 024410 (2012).

[51] R. D. Johnson, K. Cao, F. Giustino, and P. G. Radaelli, $CaBaCo_4O_7$: A ferrimagnetic pyroelectric, Phys. Rev. B **90**, 045129 (2014).

[52] S. Bordács, V. Kocsis, Y. Tokunaga, U. Nagel, T. Rõõm,

Y. Takahashi, Y. Taguchi, and Y. Tokura, Unidirectional terahertz light absorption in the pyroelectric ferrimagnet $CaBaCo_4O_7$, Phys. Rev. B **92**, 214441 (2015).

[53] V. Kocsis, Y. Tokunaga, S. Bordács, M. Kriener, A. Puri, U. Zeitler, Y. Taguchi, Y. Tokura, and I. Kézsmárki, Magnetoelectric effect and magnetic phase diagram of a polar ferrimagnet $CaBaFe_4O_7$, Phys. Rev. B **93**, 014444 (2016).

[54] R. S. Fishman, S. Bordács, V. Kocsis, I. Kézsmárki, J. Viirok, U. Nagel, T. Rõõm, A. Puri, U. Zeitler, Y. Tokunaga, Y. Taguchi, and Y. Tokura, Competing exchange interactions in multiferroic and ferrimagnetic $CaBaCo_4O_7$, Phys. Rev. B **95**, 024423 (2017).

[55] M. Valldor, Y. Sanders, and W. Schweika, High spin frustration in Co based Swedenborgites, J. Phys.: Confer. Series **145**, 012076 (2009).

[56] M. Valldor, R. P. Hermann, J. Wuttke, M. Zamponi, and W. Schweika, Spin correlations in the extended kagome system $YBaCo_3FeO_7$, Phys. Rev. B **84**, 224426 (2011).

[57] A. K. Bera, S. M. Yusuf, S. S. Meena, C. Sow, P. S. A. Kumar, and S. Banerjee, Controlling structural distortion in the geometrically frustrated layered cobaltate $YBaCo_4O_{7+\delta}$ by Fe substitution and its role on magnetic correlations, Mater. Res. Express **2**, 026102 (2015).